ISBN: 978-3-95450-253-0 ISSN: 2673-5571 doi:10.18429/JACoW-HB2023-TUA1C1

MAJOR LONGITUDINAL IMPEDANCE SOURCES IN THE J-PARC MAIN RING

Aine Kobayashi* for the MR impedance working group, KEK, Tokai, Ibaraki, Japan

Abstract

Beam intensity upgrade at the Japan Proton Accelerator Research Complex main ring is ongoing. Beam instability is controlled by feedback systems in longitudinal and transverse directions. However, in recent years, microbunch structures have been observed during debunching, inducing electron cloud, and transverse beam instability, which is a topic of concern. Thus, the cause of this problem must be identified and countermeasures must be taken accordingly. A summary of model and measurement comparisons are reported for the major impedances RF-cavities, FX-kickers, and FX-septum magnets.

INTRODUCTION

The Japan Proton Accelerator Research Complex (J-PARC) is a high-intensity proton beam accelerator facility. It consists of 400 MeV linac [1], 3 GeV rapid cycling synchrotron [2], and 30 GeV main ring (MR) synchrotron [3]. The MR supplies beams to the neutrino and hadron experimental facilities with fast (FX) and slow (SX) extractions and increases the beam power, aiming for operation at 1.3 MW in FX operation and ≧100 kW in SX operation [4].

The amount of beam loss tolerated in MR is determined by the residual dose and the limited beam intensity so it does not exceed that value. We are preparing to increase the beam intensity by adding an acceleration cavity and upgrading hardware, such as extraction equipment. However, these upgrades can lead to beam instability and preventive measures must be put in place.

Currently, longitudinal beam instability in the debunching beam has become a problem in SX operation. Microbunch structures with beam instabilty were generated at the beginning of the debunching operation. Possibly, these structures were closely related to the generation of electron clouds, transverse beam instability, and beam loss. Therefore, we are working on investigating and considering countermeasures for these concerns. This could be a problem in future FX operation candidates with time structures with low peak currents. Attempts were made to address these problem through beam manipulation, such as RF gymnastics [5], but this is not a sufficient solution. The cause of the beam instability must be investigated and countermeasures must be taken. Currently, we aim for the reduced longitudinal impedance Z_L/n to be $< 0.5\ \Omega$ in MR [6]. This value considers the Keil-Schnell criterion [7] at SX (100 kW) and the values of measured devices.

To understand the impedance of the device, measurements [8] have been made using the stretched wire method [9] and simulations have been performed using the CST wakefield solver [10].

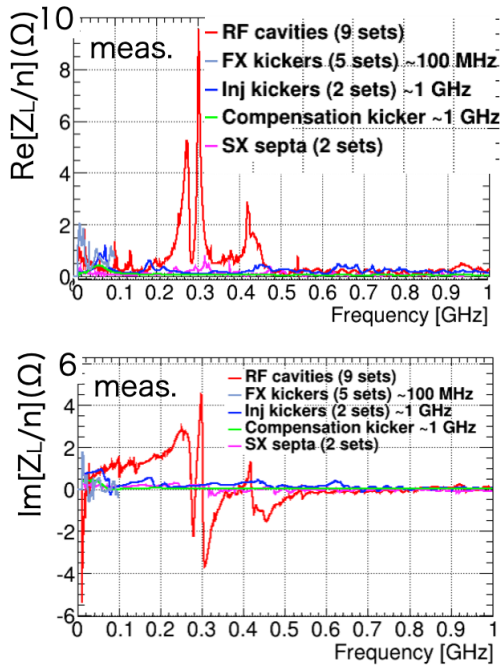

Figure 1: The major longitudinal impedance around MR.

RF CAVITIES

The MR synchrotron had seven fundamental accelerating cavities and two second-harmonic cavities to reduce space-charge effects. In the high-repetition operation started in FY2022, beam operation was started with eight accelerating cavities (fundamental) and two second harmonic cavities. To further increase the beam repetition rate, we planned to increase the number of accelerating cavities (fundamental) to 11 [4]. The accelerating cavities used in MR were made of metallic magnetic materials to achieve a high accelerating field gradient. Structurally, the cavities with four or five accelerating gaps are installed in the accelerator ring, but one gap is short-circuited in the five-gap cavity, and all cavities are basically used as four-gap cavities for beam operation. Figure 1 shows the longitudinal impedance around the ring estimated from the measurement results. From these measurements, the accelerating cavity impedance can be considereda significant contributor to the longitudinal impedance of the ring.

Simulation Model

We investigated the origin of the major resonances distributed in the 300 MHz-range shown in Fig. 1 through measurements [8] and simulations [11]. Fig. 2 shows a simula-

* aine.kobayashi@kek.jp

ISBN: 978-3-95450-253-0 ISSN: 2673-5571 doi:10.18429/JACoW-HB2023-TUA1C1

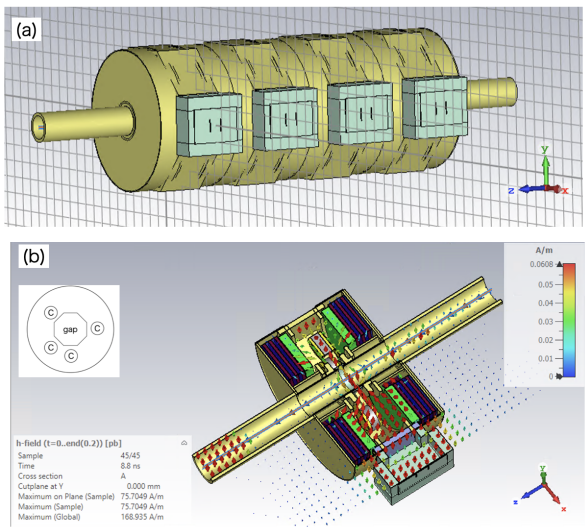

Figure 2: (a) Four-gap view of the RF cavity model; (b) electromagnetic field distribution in a single-cell cross-section.

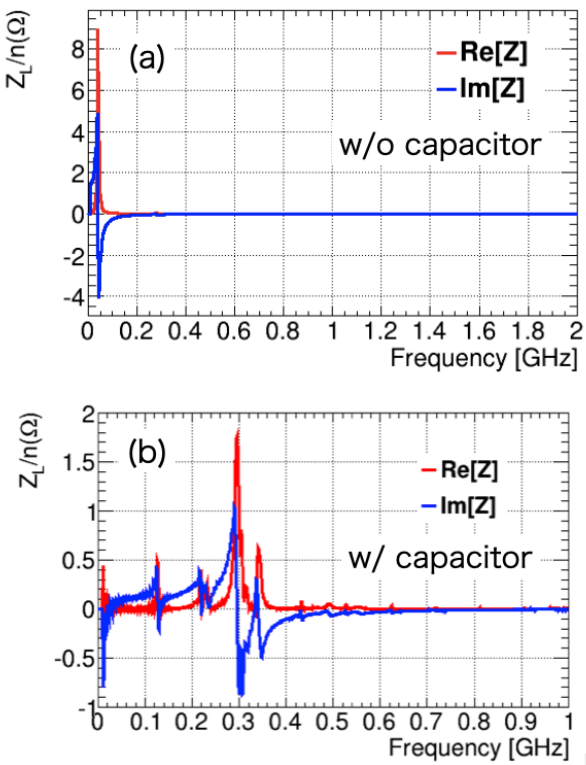

Figure 3: Longitudinal impedance of RF cavity by simulation; (a) without capacitors and (b) with capacitors (fundamental setup).

tion model of RF cavity, and this is used to better understand impedance and how to reduce it. The acceleration gap is equipped with capacitors for the fundamental and second harmonic frequencies. Figure 3 shows that the resonance moves to approximately 300 MHz in the case with capacitors (b) compared with the case without capacitors (a).

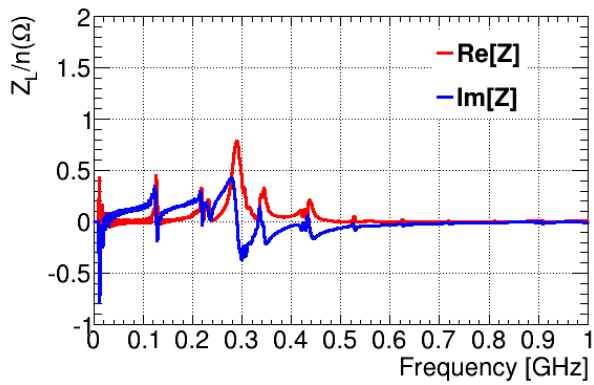

Figure 4: Simulated results of dumping resonance with analog capacitors and coils.

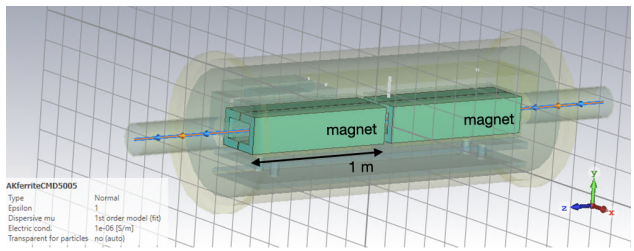

Figure 5: Simulation model of FX-kicker.

Impedance Reduction Method

As an impedance reduction plan, a method of dumping resonance with an analog capacitor and coil [12], which was also simulated using CST. The result is shown in Fig. 4, which is smaller than Fig. 3(b). Since the reduction effect is not yet sufficient, another method is under consideration.

FX-KICKERS

The FX-kicker [13] is responsible for kicking the circulating beam to the neutrino experiment line or abort line. Five FX-kickers were installed in MR and measurements were taken up to 2 GHz in 2021. Figure 5 shows CST-made model of FX kicker, and the results were calculated for five units. Figure 6 shows the calculated (a) and measured (b) impedance. The number of FX kickers will be reduced in the near future.

FX-SEPTUM MAGNETS

The FX-septum is responsible for guiding the circulating beam kicked by the FX-kicker. FX septa group configuration in the MR tunnel is shown in Fig. 7. Two low-field septum magnets of the Eddy-current type [14] and three high-field septum magnets (SM30, 31, and 32) [15] were installed in MR, which were upgraded to cope with the high intensity and high repetition rate of MR, by May 2022.

Low-field Septum Magnets

Previous low-field septum magnets installed until 2021 have been found by simulation to have a large impedance at

ISBN: 978-3-95450-253-0 ISSN: 2673-5571 doi:10.18429/JACoW-HB2023-TUA1C1

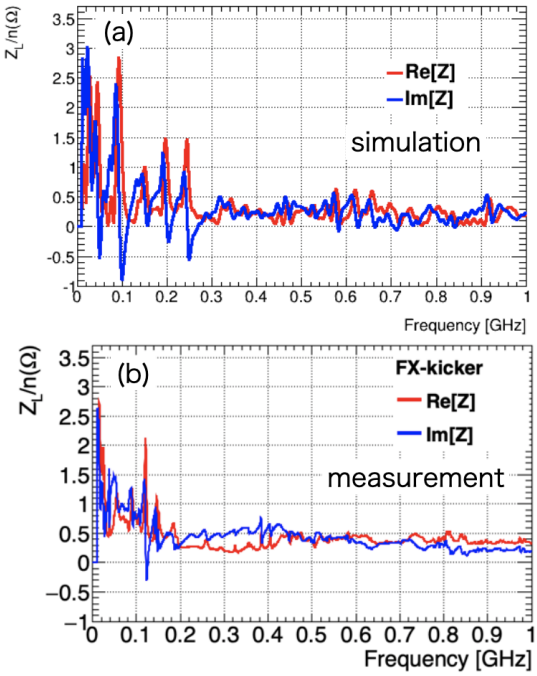

Figure 6: The longitudinal impedance for 5 FX-kickers. (a) Simulation and (b) measured values.

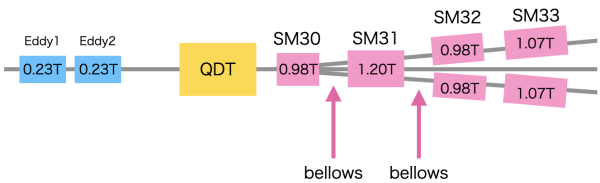

Figure 7: Schematic of the FX-septa sequence. The two upstream units are Eddy-current type septum magnets, which are low-field septum magnets, and the downstream units are high-field septum magnets across the Q-magnet.

low frequencies [16]. They were lined out at the end of 2021, and Eddy-current type septum magnets were installed. They have been in use since their operation in June 2022. However, the Eddy-current septum magnets were found to have an even larger impedance by simulation, and countermeasures have been taken accordingly [16]. This impedance was caused as a result of the wall current not flowing smoothly into the chamber containing the septum magnets, causing resonance.

If the contact is taken with a copper plate so that the wall current flows smoothly, the resonance below the cutoff frequency of the pipe is eliminated. A large value of resonance remains at this cutoff frequency. Reducing the magnitude of that remaining resonance was done using a radio wave absorber SiC.

Actual measurements and countermeasurements were taken in August 2022. Figure 8 shows the measurement result before impedance measure (a), the measurement results when contacts were made by copper plates (b) and the case where impedance was further reduced by installing

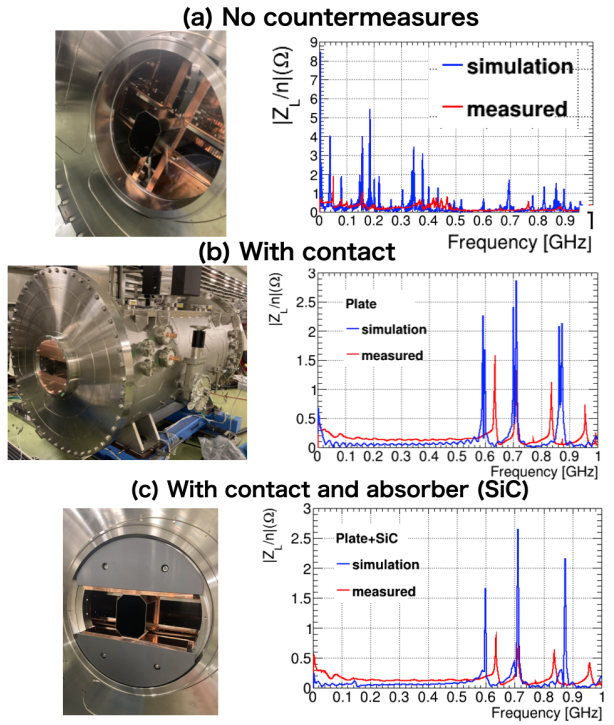

Figure 8: Comparison of the measured and simulated impedances of Eddy-type septum magnets; (a) before impedance countermeasures; (b) after installation of metal contacts as impedance countermeasures; (c) after installation of part of radio wave absorber as a further impedance countermeasure.

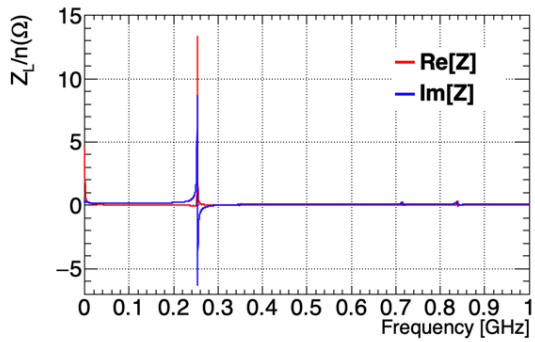

Figure 9: The measured longitudinal impedance of the high-field septum magnets SM31.

SiC blocks at one of the four locations (c). As of 2023, the situation is as shown in Fig. 8(c).

High-field Septum Magnets

There were two bellows at the connection of the three septum magnets, where the impedance was found to be high. For installation reasons, there were gaps in the beam pipe, resulting have a cavity-like structure. Each of these three septum magnets had a different impedance at different frequencies due to their different diameters. The problem is that these impedances have the same frequency and magnitude as RF cavity impedance, which we now know is a problem.

ISBN: 978-3-95450-253-0 ISSN: 2673-5571 doi:10.18429/JACoW-HB2023-TUA1C1

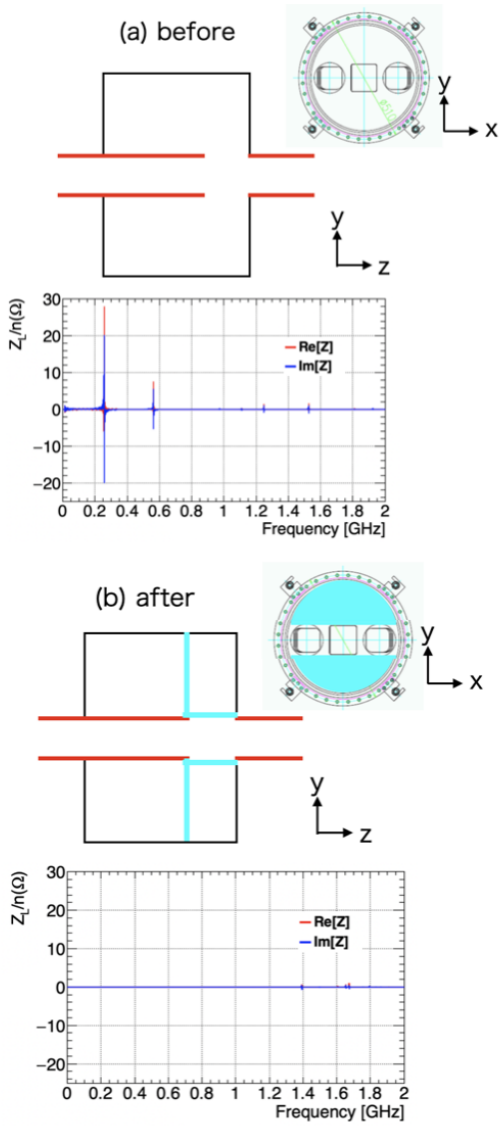

Figure 10: Example calculations of a high-field septum before (a) and after (b) impedance countermeasures.

Figure 9 shows the result for the septum magnets, including the bellows at one of the two locations measured in August 2023. This was calculated using the lumped-element formula [9]. However, extending the beam pipe to ensure the bellows' elasticity and maintainability is difficult, and we are considering installing contacts with copper plates to ensure a smooth flow of wall currents with measures similar to Eddy-current type as shown in Fig. 10.

EFFECT ON THE BEAM

The effect of the impedance of the Eddy-current type septum magnets was simulated by M. Tomizawa [6], and the effect of the countermeasures is shown in Fig. 11. The effect was seen at low frequencies below 200 MHz. This effect depends on the initial conditions and requires further investigation. In addition, the correspondence between impedance

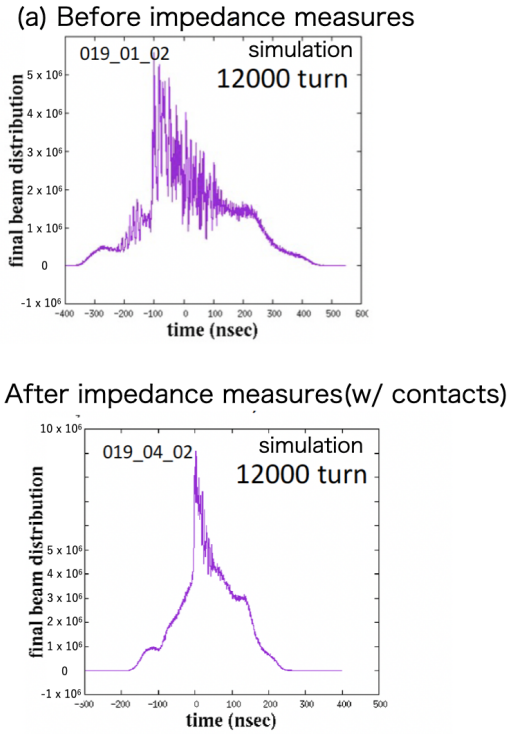

Figure 11: Simulation results of the changes in the frequency of the beam before (a) and after (b) the impedance reduction to the Eddy-type magnet septa [6].

and beam frequency is under investigation, including the effect of inductance.

Beam instability was observed at 60 kW before the impedance countermeasure. During beam tuning in SX mode in June 2023, beam instability was not observed above that intensity, and it did not occur at least up to 75 kW, where beam tuning was performed. However, as the beam conditions and RF feedback system were improved parallelly, we did not investigate whether this is due to the impedance countermeasure alone. The effect of the impedance countermeasure alone will be investigated in the future.

CONCLUSION

Upgrades are underway at J-PARC MR for beam enhancement. Microstructures in the high-intensity debunching process cause longitudinal beam instabilities, electron clouds, and transverse beam instabilities. We are in the process of measuring and addressing the major impedance sources. This report summarizes the measured and simulated impedances of the main longitudinal impedance sources, RF-cavities, FX-kickers, and FX-septa.

REFERENCES

[1] M. Ikegami *et al.*, "Beam commissioning and operation of the J-PARC linac", in *Prog. Theor. Exp. Phys.*, vol. 2012, no. 1, 2012, p. 02B002 doi:0.1093/ptep/pts019

ISBN: 978-3-95450-253-0 ISSN: 2673-5571 doi:10.18429/JACoW-HB2023-TUA1C1

[2] H. Hotch *et al.*, "Beam commissioning and operation of the Japan Proton Accelerator Research Complex", in *Prog. Theor. Exp. Phys.*, vol. 2012, no. 1, 2012, p. 02B003. doi:10.1093/ptep/pts021

[3] T. Koseki *et al.*, "Beam commissioning and operation of the J-PARC main ring synchrotron", in *Prog. Theor. Exp. Phys.*, vol. 2012, no. 1, 2012, p. 02B004. doi:0.1093/ptep/pts071

[4] S. Igarashi *et al.*, "Accelerator design for 1.3-MW beam power operation of the J-PARC Main Ring", in *Prog. Theor. Exp. Phys.*, vol. 2021, no. 3, 2021, p. 033G01. doi:10.1093/ptep/ptab011

[5] F. Tamura *et al.*, "Evaluation of higher harmonics generated in acceleration gaps during the high power beam acceleration at J-PARC RCS", in *Proceedings of the 19th Annual Meeting of Particle Accelerator Society of Japan*, Japan, Oct. 2022, pp. 175–178.

[6] Discussion in longitudinal instability meetings, M. Tomizawa, Feb. 2021, internal documents.

[7] E. Keil and W. Schnell, "Concerning longitudinal stability in the ISR", CERN, Geneva, Switzerland, Reps. CERN-ISR-TH-RF-69-48 and ISR-TH-RF-69-48, 1969. https://cds.cern.ch/record/1229157

[8] T. Toyama *et al.*, "Update of beam coupling impedance evaluation by the streched-wire method", 2022. doi:10.48550/arXiv.2208.09217

[9] E. Jensen, "An improved log-formula for homogeneously distributed impedance", CERN, Geneva, Switzerland, Rep. CERN-PS-RF-NOTE-2000-001, 2000. https://cds.cern.ch/record/960162

[10] CST - Computer Simulation Technology homepage. https://www.cst.com/products/cstps.

[11] A. Kobayashi *et al.*, "Modeling of the impedance of RF cavities in the J-PARC main ring", in *Proceedings of the 20th Annual Meeting of Particle Accelerator Society of Japan*, Chiba, Japan, Aug.-Sep. 2023.

[12] F. Tamura, internal documents.

[13] T. Sugimoto *et al.*, "Upgrade of the compensation kicker magnet for J-PARC main ring", in *Proceedings of the 9th Annual Meeting of Particle Accelerator Society of Japan*, Osaka, Japan, Aug. 2009.

[14] T. Shibata *et al.*, "The new high-field septum magnets for upgrading of fast extraction in MR of J-PARC,", in *Proceedings in the 3rd J-PARC Symposium (J-PARC2019)*, Tsukuba, Japan, Sep. 2019. doi:10.7566/JPSCP.33.011034

[15] T. Shibata *et al.*, "The new low-field septum magnet for upgrading of fast extraction in MR J-PARC (7)", in *Proceedings of the 18th Annual Meeting of Particle Accelerator Society of Japan*, Japan, Aug. 2021.

[16] A. Kobayashi *et al.*, "Impedance reduction by a SiC-loaded flange and its application to the J-PARC main ring septum magnet", *Nucl. Instrum. Methods Phys. Res., Sect. A*, vol. 1031, p. 166515, 2022. doi:10.1016/j.nima.2022.166515